Computer Simulation of Underground Blast Response of Pile in Saturated Soil

L.B. Jayasinghe*, D.P. Thambiratnam*, N.Perera*, J.H.A.R.Jayasooriya

*Science & Engineering Faculty, Queensland University of Technology, Brisbane, Australia.

ABSTRACT

This paper treats the blast response of a pile foundation in saturated sand using explicit nonlinear finite element analysis, considering complex material behavior of soil and soil-pile interaction. Blast wave propagation in the soil is studied and the horizontal deformation of pile and effective stresses in the pile are presented. Results indicate that the upper part of the pile to be vulnerable and the pile response decays with distance from the explosive. The findings of this research provide valuable information on the effects of underground explosions on pile foundation and will guide future development, validation and application of computer models.

Key words: underground explosion; numerical simulation; pile foundation, saturated soil

1. INTRODUCTION

Increasing terrorist attacks have led to greater scrutiny of the design of structures to random and unexpected loads such as impacts and blasts. In order to design structures to withstand blast loading, it is necessary to ensure the design is suitable for the level of risk and adheres to the appropriate standards. The understanding of blast effects on piles, combined with structural damage data from historical explosions, as well as information from research on the response of structures under blast loading enables the evaluation of the effectiveness of current design standards and practices.

The performance of underground structures subjected to blast loads is a critical research area, as these structures play an important role in the overall structure response. Underground explosions usually produce a crater, and blast-induced ground shock propagates in the surrounding soil media. If an explosion occurred near a buried structure, the soil pressure and

acceleration will result in severe damage or even the collapse of the structure. Therefore, ground vibrations resulting from underground explosion are of great interest to engineers who deal with the design of underground structures.

Although pile foundation is a surface buried structure, it can be assumed as an underground structure in some aspects. Pile foundations transfer the large loads from the superstructure above into deeper, competent soil layers which have adequate capacity to carry these loads. It follows that if these foundations are structurally damaged due to blast loading, the superstructure becomes vulnerable to failure. Despite the importance of blast response of pile foundation, only a few publications can be found in literature, probably due to the complexities in the material behavior of the soil and the soil-pile interaction.

Many studies have been done on the propagation of blast induced waves in the air, soil and rocks [1-3]. The evolution of centrifuge tests had led to many studies on the dynamic response of underground structures under blast loading [4, 5]. Shim [6] used centrifuge models to study the response of piles in saturated soil under blast loading. However, with the rapid development of computer programs, it has become possible to carry out detailed numerical simulations of response of underground structures under buried blasts [7, 8] and study the effects of controlling parameters. Some past studies have used centrifuge test results to compare Finite Element (FE) model results [9-15]. Anirban De [9] used numerical simulations with ANSYS Autodyn 13 to study the effects of a surface explosion on an underground tunnel using a 3D Finite Element model. A fully coupled Euler –Lagrangian formulation was used to model fluid-structure interaction under blast loading. His model was verified through typical model tests using geotechnical centrifuge. This has provided confidence in the procedure used herein.

This paper treats the response of pile foundation to a buried blast loading using numerical simulations through the commercial software package LS-DYNA [16]. The present study adopts the fully coupled numerical simulation approach. A brief description of the background on modeling is presented at the beginning of this paper. Then, the blast wave propagation in soil and the response of a pile to underground explosions are presented. Results from the numerical modeling are validated using those from the centrifuge tests reported in Shim's study [6].

2. PROBLEM DESCRIPTION

Tests on the centrifuge model described in Shim's [6] study, are considered in this paper. Shim carried out a series of 70-g centrifuge tests to investigate the blast wave propagation and response of piles embedded in saturated sand. The corresponding prototype model dimensions are used for the numerical simulation. Granier et al [17] have developed required similitude principles and scaling laws to extrapolate model dimensions to prototype dimensions. Table 1 presents the scaling laws for common parameters which link the model to an equivalent prototype with respect to a centrifuge acceleration of Ng, where N is the scale factor and g is the acceleration due to gravity. For example a 1kg charge in a model subjected to 70-g's is equal to 343 ton (or 70^3kg) of prototype (full scale) explosives. Figure 1 compares the stresses and strains of a prototype and a 1/N scale centrifuge model. It can be seen that the stresses and strains are equal in both prototype and the centrifuge model.

Table 1. Scaling laws [18]

Parameter	Model at N-g's	Prototype value
Length	1/N	1
Area	$1/N^2$	1
Volume	$1/N^3$	1
Mass	$1/N^3$	1
Velocity	1	1
Acceleration	N	1
Force	$1/N^2$	1
Pressure	1	1

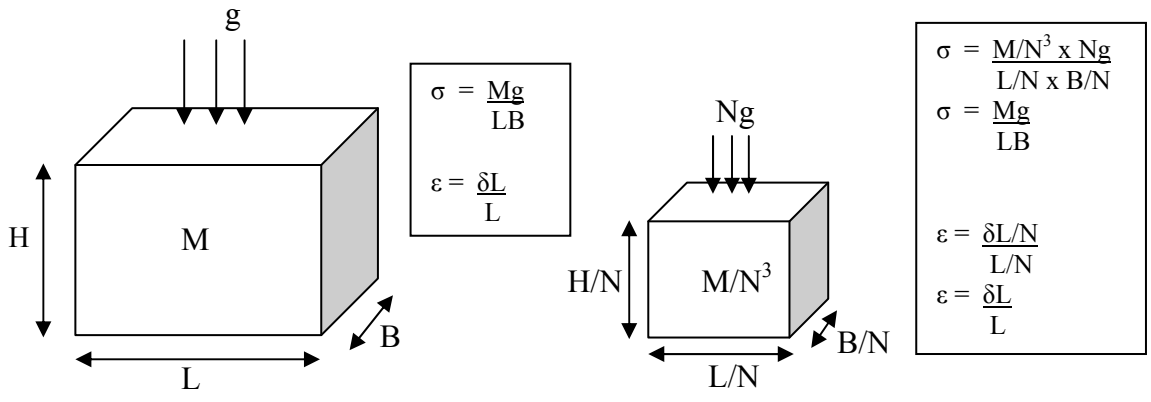

(b) Prototype (a) Centrifuge model

Figure 1. Stress similarity in prototype model and centrifuge model

The finite element models are developed for considering an aluminum pile of 10m length (it corresponds to 14.3cm in centrifuge model dimension) with hollow circular cross section. Table 2 shows the pile's dimension and properties. Configuration of a generic scenario is shown in Figure 2. The cylindrical shape blast source is considered at mid depth of the soil (i.e. 5m from top surface) and distance between pile and explosive is equal to 7.5m.

Table 2. Dimensions and properties of Aluminum pile

Description	Value
Outer diameter	400 mm
Inner diameter	335 mm
Thickness	65 mm
Alloy and Temper	3003 H-14
Modulus of elasticity	71 Gpa
Ultimate tensile strength	150 Mpa
Yield Strength	145 Mpa

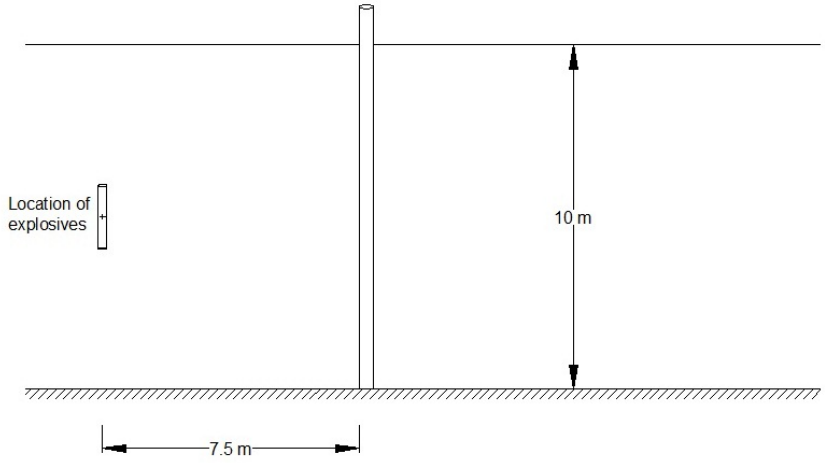

Figure 2. Configuration of a generic scenario

3. APPROACH

This study was carried out using dynamic computer simulation technique. Finite element modeling code LS-DYNA was used for the computer simulation. Considering the symmetries of the geometrical model as shown in Figure 2, to save computation time, a quarter of the air

domain, soil domain and explosive and half of the pile were modeled as shown in Figure 3 which shows the five different parts. Eight node solid elements were used for all parts in the FE model for the 3D explicit analysis. The global uniform mesh size was set to be 25cm in the model. However, Pile was meshed with 25mm long, 8-node hexagonal brick elements.

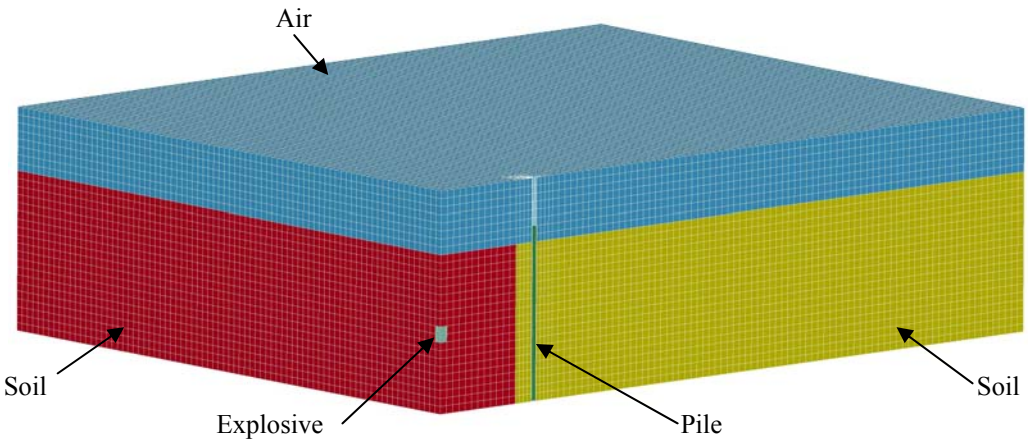

Figure 3. Finite element model

Eulerian meshes were generated for the explosive, air and for a part of soil that is relatively close to the explosive. This is to eliminate the distortion of the mesh under high strains. On the other hand Lagrangian meshes were used to model the rest of the system including the pile and the soil region away from the explosive. In the Lagrangian method, the numerical mesh moves and deforms with the physical material. No material passes between elements. As all the material is contained in their original cells, time dependent material properties can be well described. The main disadvantage of a Lagrangian method is that severe mesh distortion can occur as the mesh deforms with the material, and this can lead to erroneous results or termination of an analysis. In contrast to a Lagrangian analysis, an Eulerian analysis involves material flow through a stationary mesh. As the mesh is fixed, there is no mesh distortion problem when large deformations occur. However, the Eulerian method is computationally more expensive than the Lagrangian method and hence an appropriate mix of both methods is used. Thus, soil is modelled with both Eulerian and Lagranigan meshes to address the above shortcomings. The 1-point multi material ALE solver (ELFORM=11) was used for the explosive, air and near field soil, while the default constant stress solid formulation (ELFORM=1) was used for the pile and far field soil elements. The materials of

the explosive, air and near field soil are specified as multi material using LS-DYNA multi material capabilities (*ALE_MULTI_MATERIAL_GROUP).

In the presented numerical simulation, blast pressure is applied to the pile foundation indirectly. Blast pressure is generated by an LS-DYNA algorithm, which utilizes the equation of state for high explosives. The JWL (Jones-Wilkin-Lee) Equation of State (EOS) was used with the high explosive material model to model the H6 explosive. The JWL equation of state defines the pressure as a function of the relative volume, V and initial energy per volume, E, such that [16]

$$P = A\left(1 - \frac{\omega}{R_1 V}\right)e^{-R_1 V} + B\left(1 - \frac{\omega}{R_2 V}\right)e^{-R_2 V} + \frac{\omega E}{V} \qquad \text{Eq. 1}$$

Where, A, B, R_1, R_2 and ω are constants pertaining to the explosive.

In the high explosive burn material model, an EOS is used where the burn fractions, F, controls the chemical energy release for detonation simulations. The burn fraction is taken as [16]:

$$F = \max(F_1, F_2) \qquad \text{Eq. 2}$$

Where

$$F_1 = \frac{2(t - t_l)D}{3\Delta x} \qquad \text{Eq. 3}$$

$$F_2 = \frac{1 - V}{1 - V_{cj}} \qquad \text{Eq. 4}$$

In the above equations, D is the detonation velocity, ρ is the density, V_{cj} is the Chapman-Jouget volume, V is the relative volume, t_l is lighting time, t is the current time and Δx is characteristic length of element [16].

If the burn fraction, F, exceeds unity, it is reset to one and is held constant. The high explosive pressure, P, in an element is scaled by the burn fraction such that:

$$P = F.P_{EOS} \qquad \text{Eq. 5}$$

In the above equation P_{eos} is the pressure from an EOS (Eq. 1). Table 3 shows the material constants and EOS parameters used for the H6 explosive [19].

Table 3. Material model and EOS parameters of the H6 explosive [19]

ρ (kg/m^3)	**v_D (m/s)**	**P_{CJ} (Mpa)**	**A (GPa)**	**B (GPa)**
1760	7470	24	758.07	8.513
R_1	**R_2**	**ω**	**V**	**E_0 (GPa)**
4.9	1.1	0.2	1	10.3

The air is modeled using null material model with a linear polynomial EOS, which is linear in internal energy per unit initial volume, *E*, and the pressure *P*, is given by [16]

$$P = C_0 + C_1\mu + C_2\mu^2 + C_3\mu^3 + \left(C_4 + C_5\mu + C_6\mu^2\right)E \qquad \text{Eq. 6}$$

In the above equation, C_0, C_1, C_2, C_3, C_4, C_5, and C_6 are constants and $\mu = \frac{\rho}{\rho_0} - 1$, where $\frac{\rho}{\rho_0}$ is the ratio of current density to initial density. Table 4 shows the parameters used in the air model.

Table 4. Material model and EOS parameters of air

ρ (kg/m^3)	**C_0**	**C_1**	**C_2**	**C_3**	**C_4**	**C_5**	**C_6**	**E_0 (MPa)**
1.29	0	0	0	0	0.4	0.4	0	0.25

The pile is modeled using piecewise linear plasticity material model with the material properties of Aluminum alloy 3003 H-14 is given in Table 2. Density and Poisson ratio are taken as 2727 kg/m3 and 0.33, respectively for the Aluminum pile.

Upon evaluation of available soil material models in LS-DYNA, *MAT_FHWA_SOIL model was found most appropriate to model the fully saturated sand. This material model was chosen as it includes strain softening, kinematic hardening, strain rate effects, element deletion, and most importantly excess pore water effects [16], which was necessary since

saturated sand was considered in this study. Specific gravity and void ratio of the soil are taken as 2.65 and 0.67, respectively, and the equations in the LS-DYNA theory manual were used to determine the input parameters. The input card for the soil material model 147, which was used to model saturated soil in this research is shown in Figure 4. It presents the densities of soil and water, bulk modulus, shear modulus, friction angle and cohesion of soil, etc.

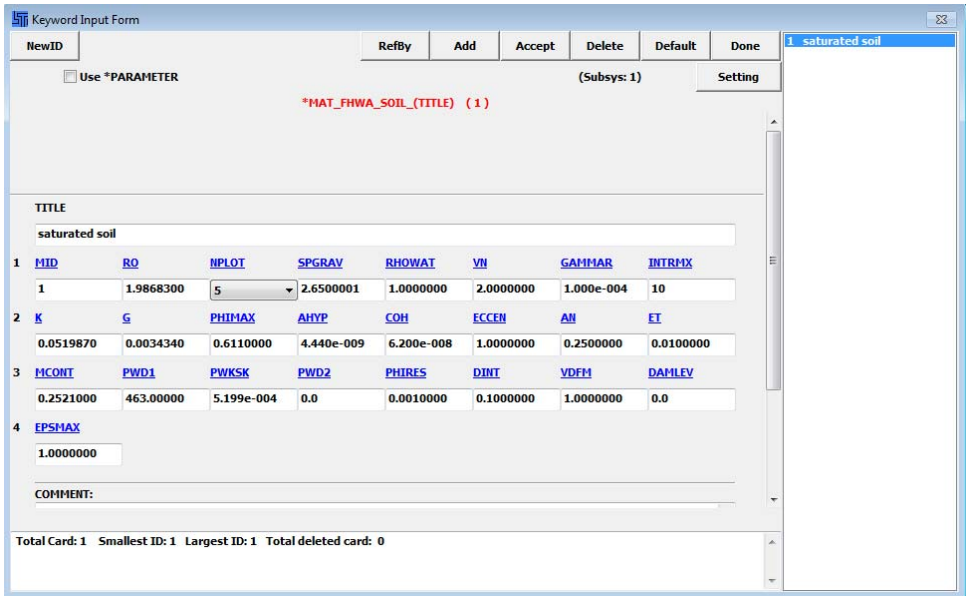

Figure 4. LS-Prepost input card for soil material parameters

PWD1 is a constant relating the stiffness of the soil material before the air voids collapse. In fully saturated soil, Lee [20] estimated this parameter to be 4.63 per GPa. PWD2 is a parameter for pore water pressure before the air voids collapse. Lee [20] showed that PWD2 has no effect on pore water pressure in fully saturated soil. As strain softening (damage) increases, the effective stiffness of the element can become very small, causing severe element distortion. One solution to this problem is deleting these distorted elements. DAMLEV is the percentage of damage, expressed as a decimal that causes the deletion of an element. EPSMAX is the principle failure strain at which the element is deleted. It is important to note that both DAMLEV and EPSMAX must be exceeded in order for element deletion to occur [21]. Lee [20] recommended a value of zero (no deletion) as he found that when elements are deleted from a model a detrimental shock wave is produced. Thus element deletion is not considered in this study. Full explanation on the input card can be found in the LS-DYNA user manual [16].

Contact between the soil and the pile was modeled with the automatic surface to surface option in LS-DYNA. Although the FE model was generated with cuboid-shaped meshes, the explosive was contained within the soil mesh by specifying an initial fraction of the soil volume to be occupied by the explosive using the Initial_volume_fraction_geometry option in LS-DYNA. This option is used in conjunction with the ALE multi material formulation. The explosive geometry can be specified as a sphere, a cylinder or a cube. This option is very useful as it allows the user to model different shapes for the explosive without changing the model mesh. Sherker [22] has shown that this method gives the best results for blast wave pressures in air and compares well with values calculated using UFC-3-340. Thus, a cylindrical explosive was defined by specifying its origin and radius.

Furthermore, the bottom of the mesh which represents the bed rock was considered as fixed in all directions. All symmetry faces are fixed against translational displacements normal to the symmetry planes. Non reflecting boundaries are applied to the other two lateral surfaces and the free boundary condition is used for the top surface. Pile top is considered as fixed in all directions. The model is subjected to gravity load to provide the hydrostatic pressure and energy on the overburden soil body. The axial load acting on the pile was not considered in this study, as was the case with the fixed end case treated in the centrifuge test [6].

4. RESULTS AND DISCUSSION

Two finite element models are developed, and one was without the pile to validate the free field stresses in soil and the other was with a pile to evaluate pile response for a buried explosion. These finite element models were developed considering the prototype dimensions, where the soil is 10m high and the explosion occurs at 5m depth.

Analysis of the FE model (of the soil and pile) was to be carried out for 2 seconds duration. Using the High Performance Computing facilities at the Queensland University of Technology, simulation took 13 hours to solve when using four parallel processors. The simulations were conducted in two steps in the model with the pile. The first step was stress initialization to induce steady pre-stress in the model using DYNAMIC_RELAXATION option in LS-DYNA. Due to this dynamic relaxation, stresses in the soil and pile act as initial

conditions for the blast analysis. Stress distributions at 600ms show that the model is initialized as shown in Figure 5. The convergence and kinetic energy curves for dynamic relaxation are shown in Figure 6(a) and 6(b), respectively. The explosion was initiated as the next phase after the dynamic relaxation phase. The soil-pile response was analyzed in this phase, and the results are discussed in the following sections.

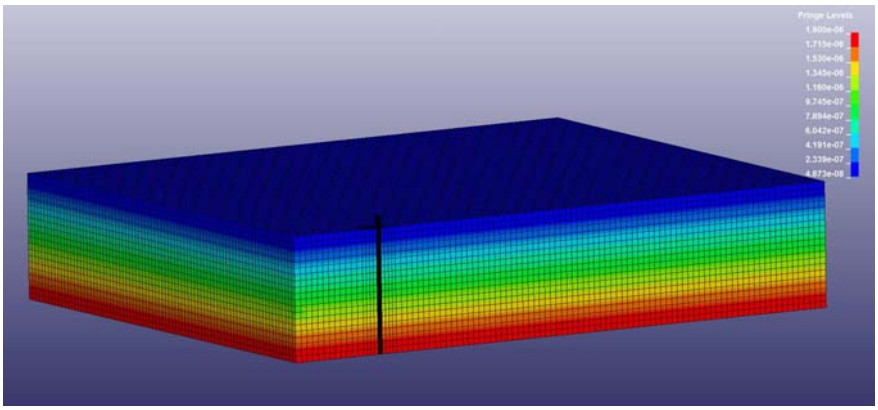

Figure 5. Stress Initialization at 600ms in the model

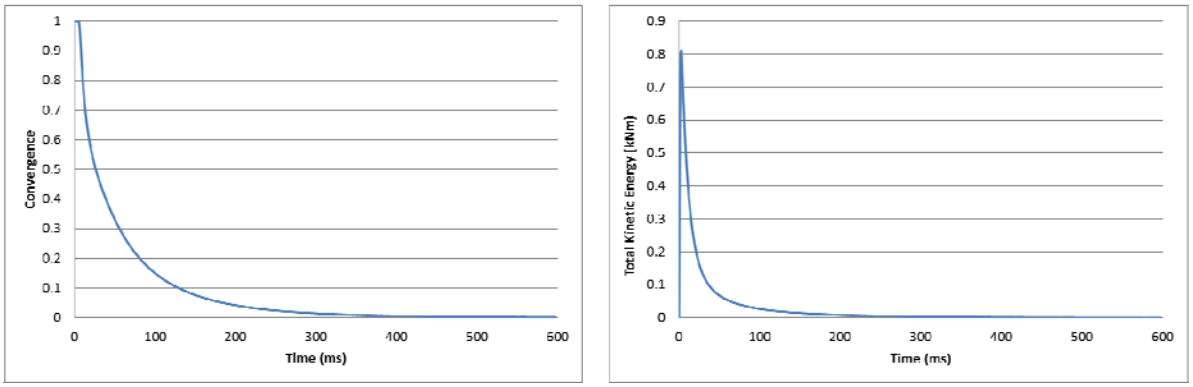

(a) (b)

Figure 6. (a) Convergence vs. Time (b) Kinetic energy vs. Time

4.1. Blast wave propagation through soil

Figure 7 shows the progressive wave propagation in the soil at different time incidents. It demonstrates that the pressure waves propagate in the soil in the form of hemispherical waves, with the area of wave front increasing with the wave propagation.

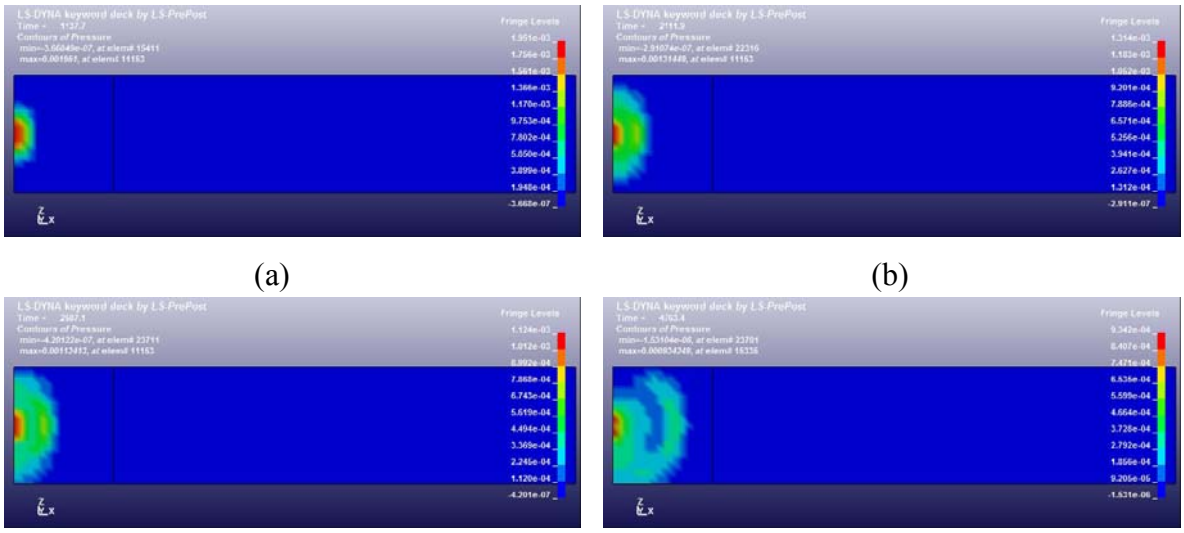

(a) (b)

(c) (d)

Figure 7. Pressure contours in the soil at different times
(a) 1.14ms (b) 2.1ms (c) 2.59ms (d) 4.76ms

Stress time histories of the compressive waves at different points in the soil located at 5, 7.5, 10, 12.5, 17, 20 and 25m (measured horizontally) from the charge are presented in Figure 8. The propagation and the attenuation of these waves can be clearly seen in this Figure in which the explosive wave pressures are high in the vicinity of the charge and they decrease with the increase of distance.

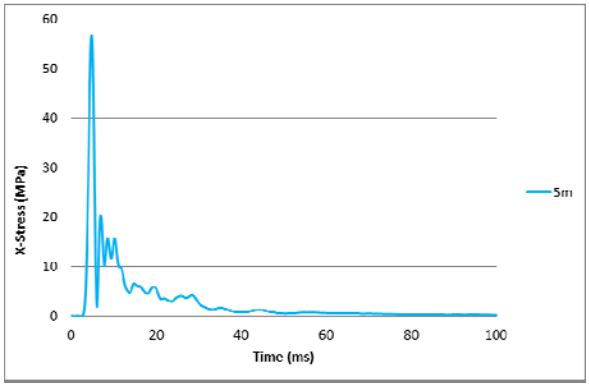

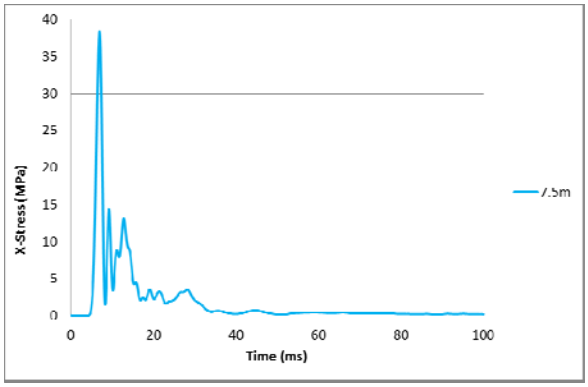

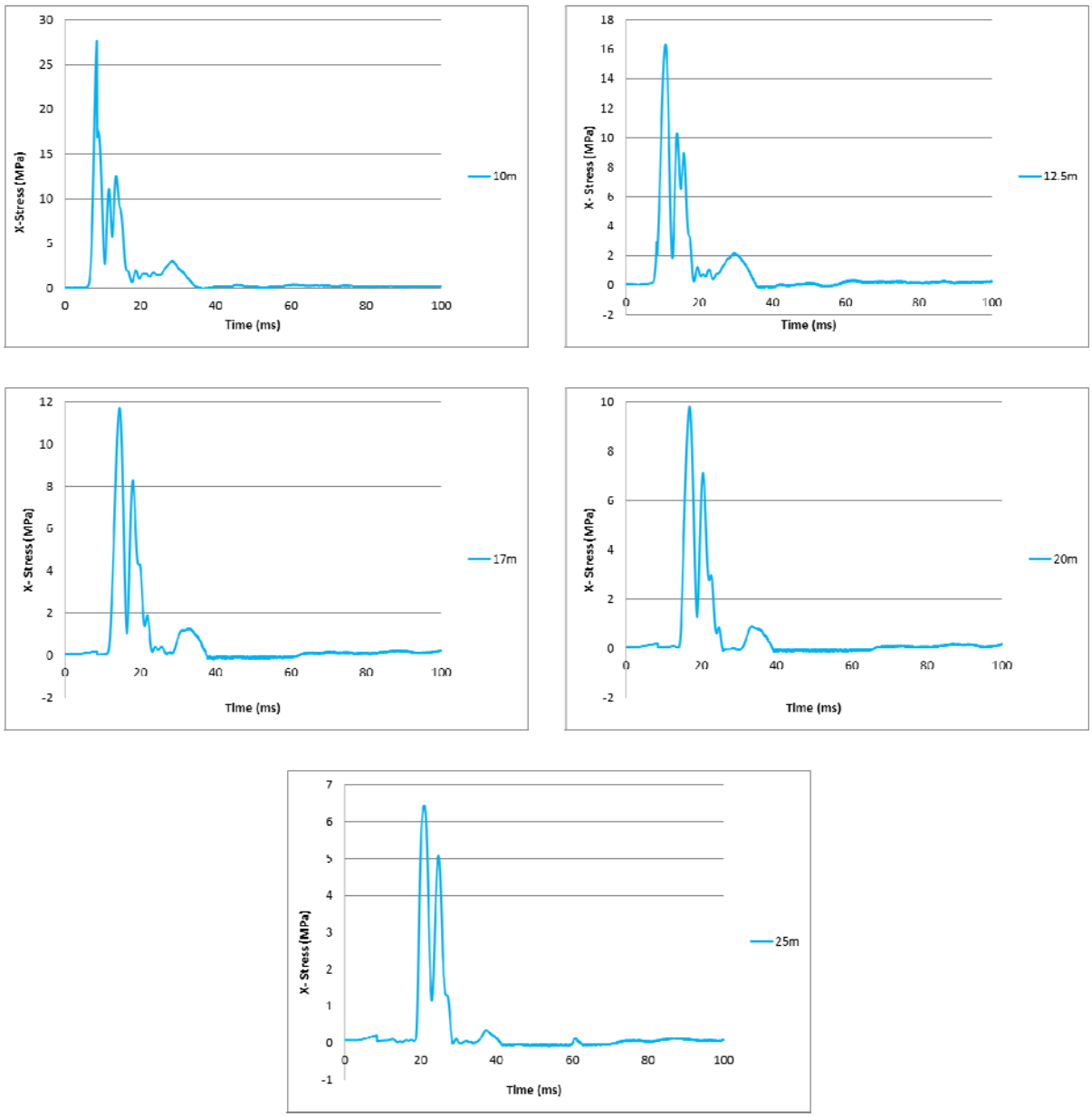

Figure 8. Stress time history at different distances in soil from charge

These results for the free field stresses in the soil correspond to the experimental results of Shim [6] obtained at 7.1, 10.7, 14.3, 17.9, 24.3, 28.6 and 35.7cm respectively. Figure 9 shows the peak stress vs. distance plots from the present numerical analysis and those from the Shim's [6] study. It can be seen that Shim's [6] experimental results are marginally higher than the present numerical results. This is due to the confinement of charges. The casing of the bomb was not included in the present model, which considered a bare charge in the

simulations. Nevertheless, the two sets of results agree reasonably well and provide confidence in the present numerical model.

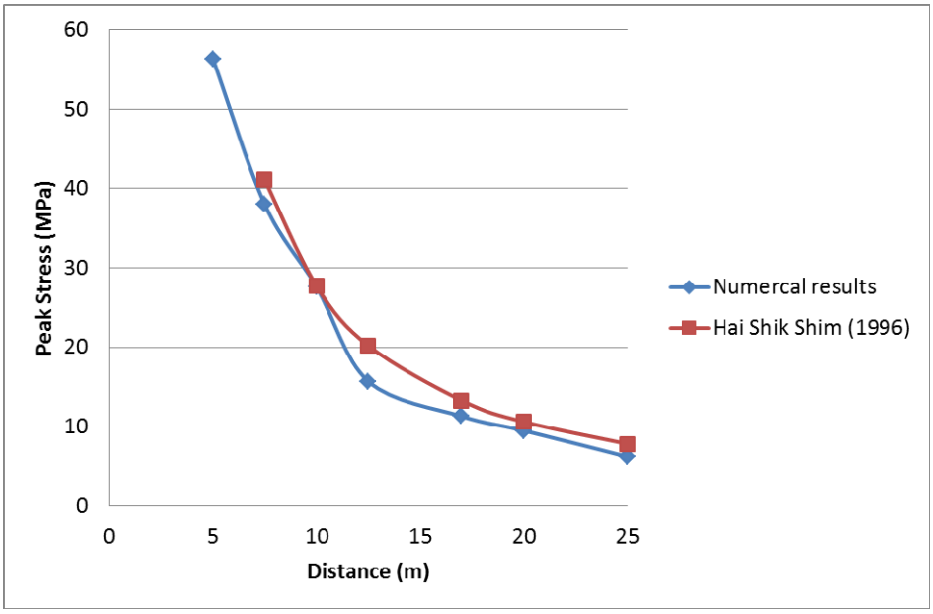

Figure 9. Comparison of free field stresses in soil

4.2. Response of pile

Considering standoff distances (distance from the detonation point to the pile) of 7.5m, 12.5m and 17m, pile responses were analyzed to compare the results with the corresponding results from centrifuge tests [6] and hence to validate the model. The horizontal deformation and acceleration of pile and the effective stress on the pile were obtained at 7 monitoring points on the pile as shown in Figure 10.

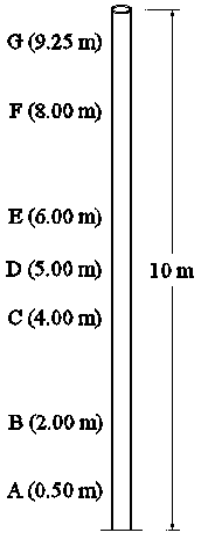

Figure 10. Monitoring points on the pile

Figure 11 shows the time histories of the horizontal deformation of the pile at the 7 monitoring points for a stand-off distance of 7.5m (from the explosive). It demonstrates that the pile has suffered permanent deformation under the buried blast and the maximum residual deformation of 254mm, occurs at the monitoring point E located 6m above from the pile tip (Figure 9). These residual deflections show the occurrence of plastic deformation of the pile under the effect of the blast loads.

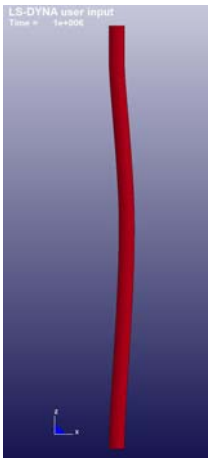

(a)

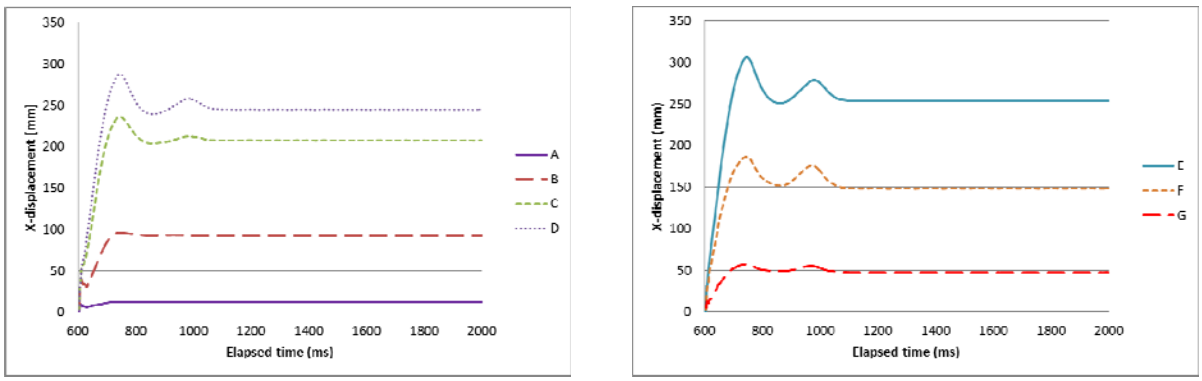

(b)

Figure 11. (a) Pile deformation (b) Horizontal displacement vs. Elapsed time at seven points

Figure 12 is the comparison of residual horizontal deformations of the pile along its height obtained from the present analysis, for this stand-off distance, and the corresponding prototype values from the experimental results of Shim [6]. The proximity of the two curves

indicates a reliable correlation between the present numerical results and the experimental results of the Shim [6].

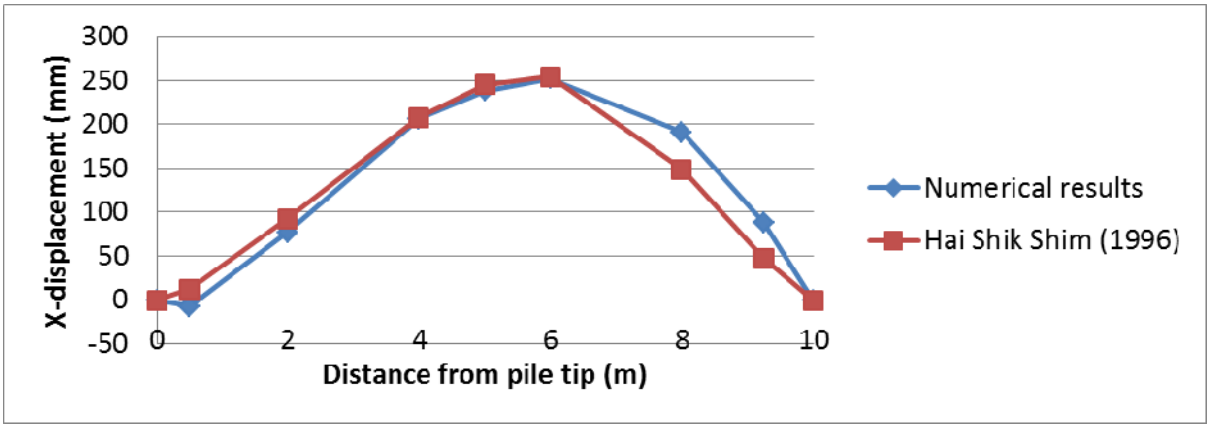

Figure 12. Comparison of Horizontal deformation of pile

Figure 13 shows the residual horizontal pile deformations of the pile along its height for the stand- off distances of 12.5m and 17m from the explosion. It shows that the pile response has decreased with the increase of distance from the charge, as expected, due to the attenuation of the compressive waves in the soil as seen in Figure 7.

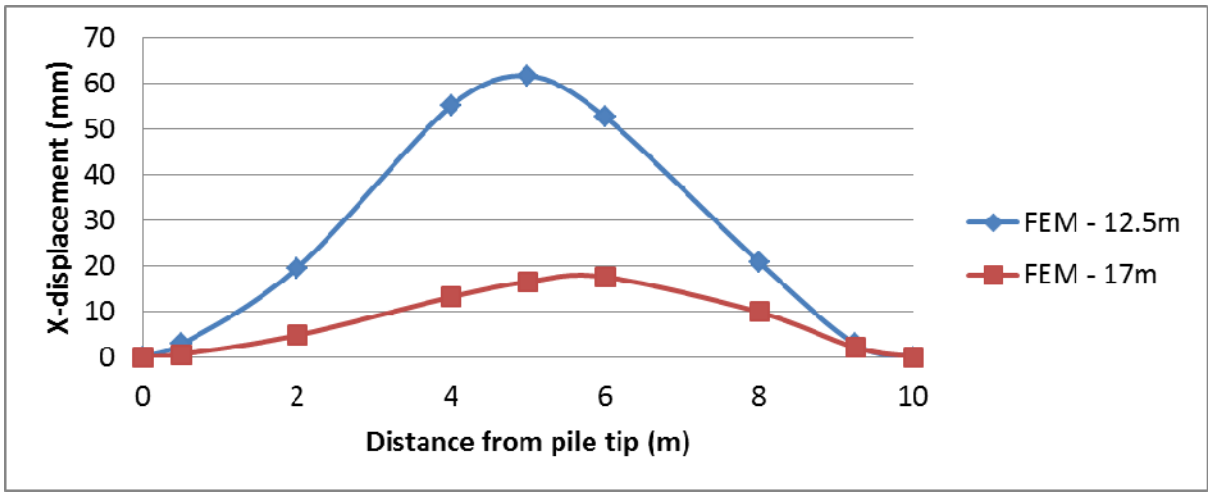

Figure 13. Horizontal deformation of pile at 12.5m and 17m distance from explosion

In Figure 14, the horizontal residual deformations of the pile along its height, obtained in the present study for all 3 stand-off distances are compared with those from reference [6]. It is evident that the pile response decays dramatically with the stand-off distance or distance from the explosive. It is also clear that results obtained from the present numerical simulations

show good agreement with the corresponding prototype values of the experimental results in [6]. For the stand-off (charge) distance of 17m, no significant permanent displacements were experienced. These results on the pile response provide adequate confidence in the present modeling techniques.

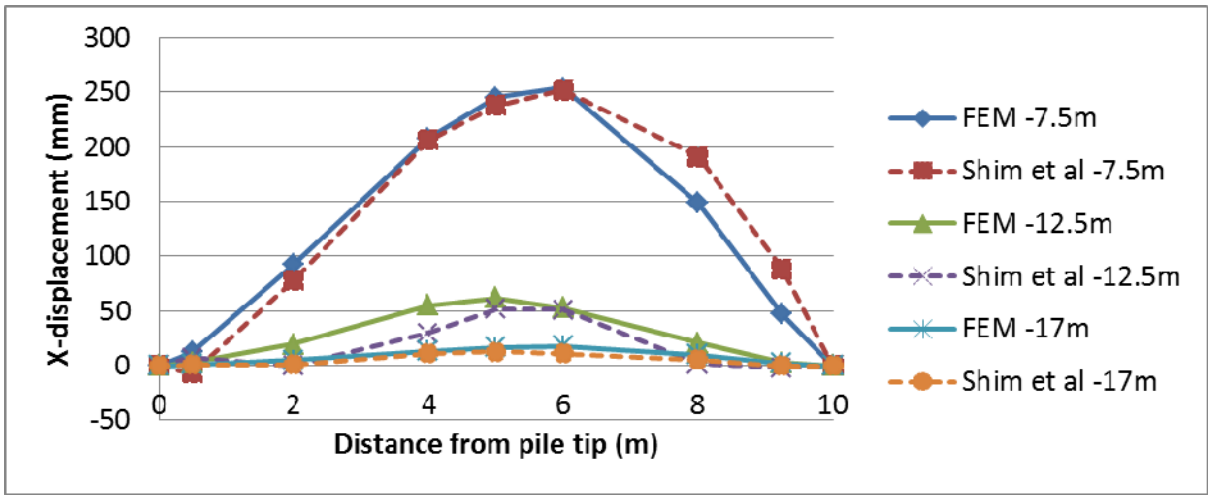

Figure 14. Comparison of Horizontal deformation of piles

Figure 15 shows the horizontal acceleration response at the monitoring point D on the pile (Figure 9), which reflects the features of high amplitude, short duration and fast attenuation under the blast induced waves.

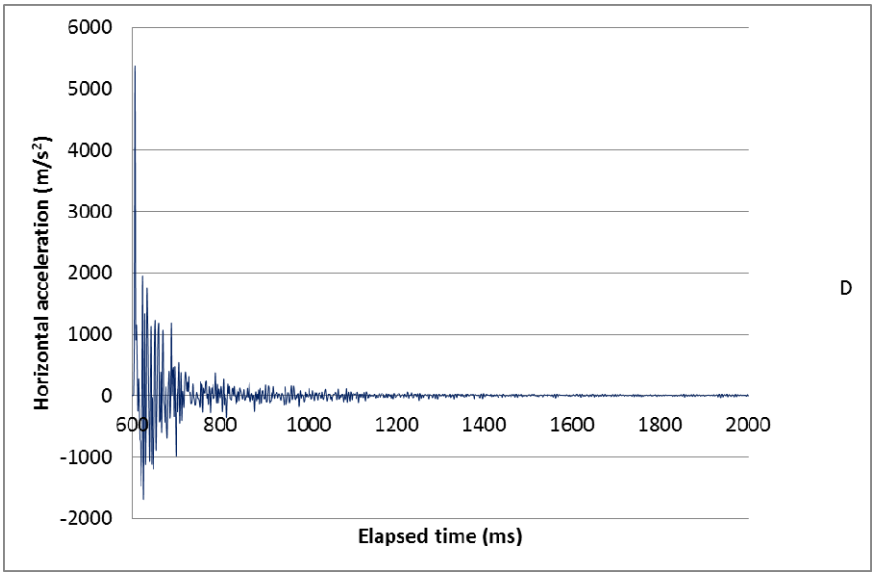

Figure 15. Horizontal acceleration of pile at point D

Figure 16 shows the effective stress response of the pile for a stand-off distance of 7.5m (from the charge). Figure 16(a) demonstrates that the pile has yielded at the ends and middle (on the side opposite to the blast load). Figure 16(b) shows maximum effective stresses at the seven monitoring points on the front face of the pile. It is clear that the pile stresses at the monitoring points A, E and G have reached the ultimate strength of 150MPa. It hence evident that the upper part of the pile (E to G) seems more vulnerable compared to the rest of the pile. Based on these observations, it is likely that the pile would fail.

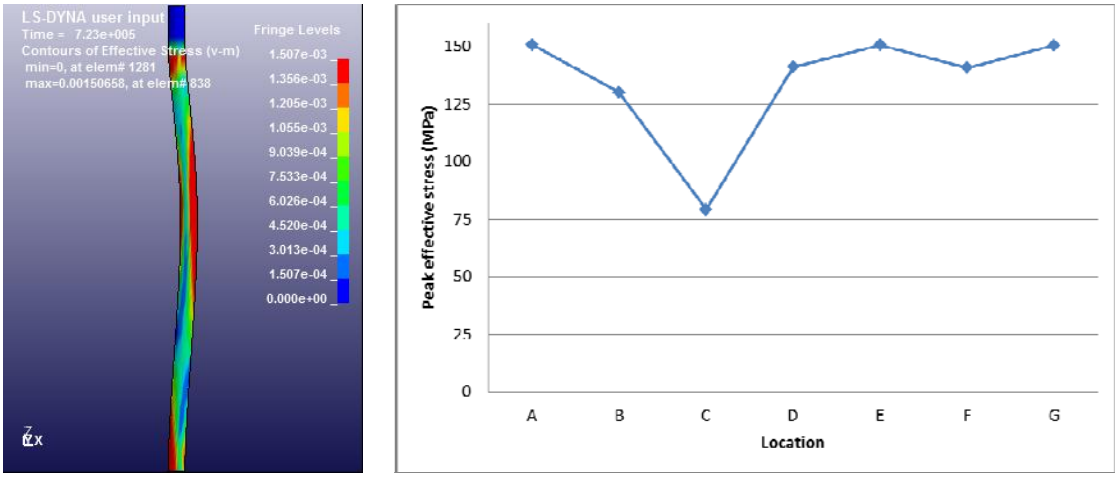

(a) (b)

Figure 16. (a) Contours of effective stress (b) Peak effective stresses on the pile

5. PARAMETRIC STUDY ON EFFECT OF CHARGE WEIGHT

In order to study the effect of explosive weight on the pile response, analyses were carried out using the same finite element model and material parameters. However, as explained earlier (in section 3) Spherical TNT explosives were considered instead of cylindrical H6 explosive for the parametric study. Table 5 shows the material constants and EOS parameters used for the H6 explosive [23]. The horizontal deformations of pile for explosive charges from 100 to 500 kg TNT situated at the mid depth of the soil and at varying distances from the pile were determined.

Table 5. Material model and EOS parameters of the TNT explosive [23]

ρ (kg/m^3)	**v_D (m/s)**	**P_{CJ} (Mpa)**	**A (GPa)**	**B (GPa)**
1630	6930	21	373.8	3.747
R_1	**R_2**	**ω**	**V**	**E_0 (GPa)**
4.15	0.9	0.35	1	6

Altogether seven load cases were considered as shown in Table 6. First 5 cases are used to determine the effect of charge weight on the results for a constant stand-off distance if 7.5m, while the last 3 cases are used determine the effect of stand-off distance on the results.

Table 6. Load cases

case	Distance (cm)	TNT charge (kg)
1	7.5	100
2	7.5	200
3	7.5	300
4	7.5	400
5	7.5	500
6	12.5	500
7	17	500

Figure 17 shows the variations of the residual horizontal displacements at the seven monitoring points (Figure 10) on the pile for load cases 1 to 5. As expected, the results indicate that pile deformations increase with charge weight. It can be seen that point E has the maximum pile deformations in all cases and that this maximum displacement for case 5 is approximately 5 times that for case 1.

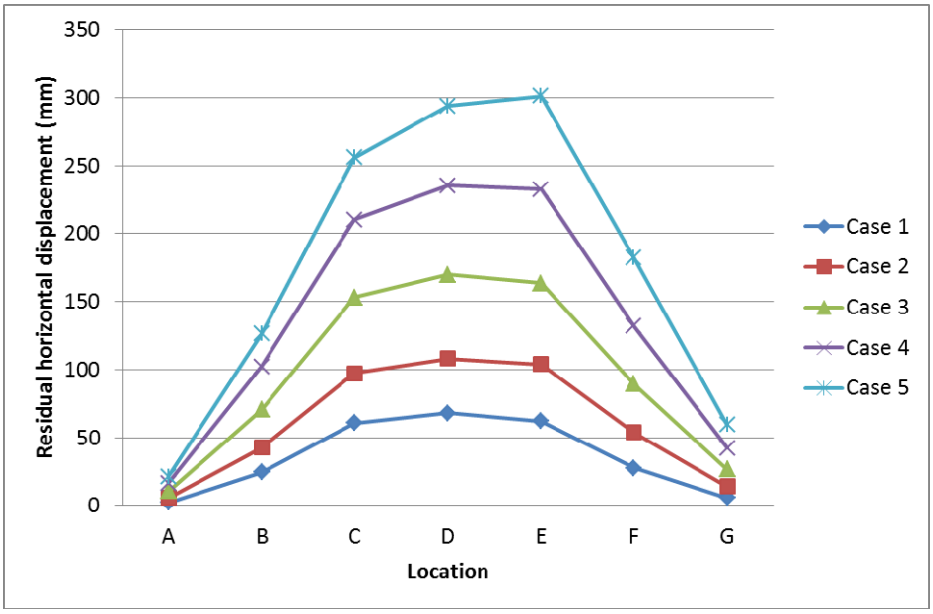

Figure 17. Comparison of five cases at seven points

Figure 18 shows the comparison of the residual horizontal displacements at the seven monitoring points (Figure 10) on the pile for cases 5 to 7. It is evident that peak values of these horizontal displacements occur at point E and that they decrease with the distance from the charge, as expected.

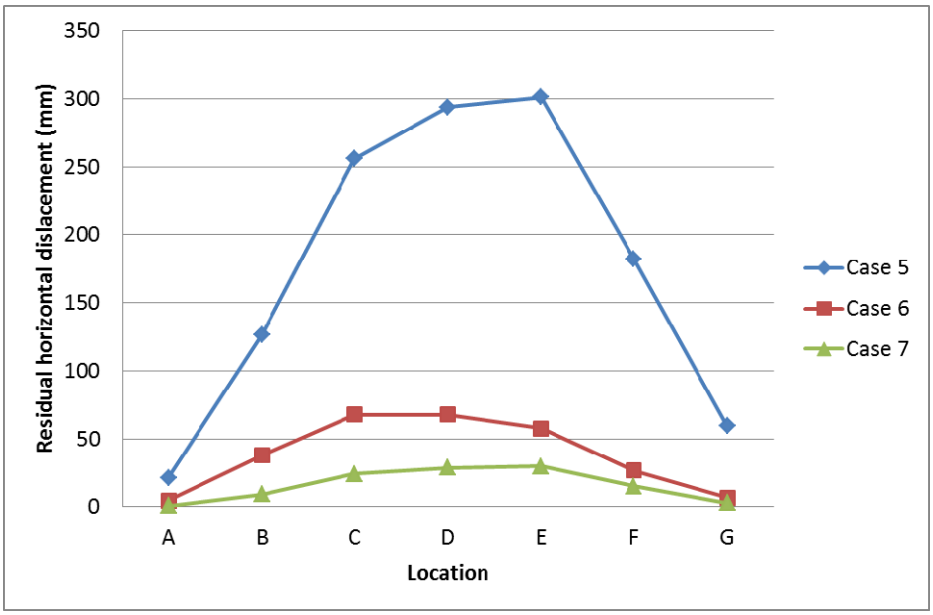

Figure 18. Comparison of three cases at seven points

6. SUMMERY

The dynamic response of pile foundation to a buried explosion has been evaluated using the commercial computer program LS-DYNA. The numerical simulation results show the compressive stresses in the soil are high in the vicinity of the charge and they decrease with increase of distance. Peak pressures in the soil and the horizontal pile displacements of the pile obtained from the present numerical simulations are compared with the experimental results in reference [6] and show good agreement. This provides adequate confidence in the modeling techniques used in this study which could then be extended. The numerical results indicate that the upper part of the pile is vulnerable, and the pile response decays dramatically with the distance from the explosive. The findings of this study will guide future development, validation and use of numerical models for treating blast responses of embedded piles.

7. REFERENCES

[1] J.L. Drake, and C.D. Little, Ground shock from penetrating conventional weapons, Proc. 1st Symp. On the interaction of non-nuclear munitions with structures, US Air force academy, CO, 1983, pp 1-6.

[2] P.S. Westine, and G.J. Friensenhahn, Free-field ground shock pressure from buried detonations in saturated and unsaturated soils, Proc. 1st Symp. On the interaction of non-nuclear munitions with structures, US Air force academy, CO, 1983, pp 12-16.

[3] C. Wu, Y. Lu, and H. Hao, Numerical prediction of blast induced stress wave from large scale underground explosion, International journal for numerical and analytical methods in geomechanics, 28 (2004), pp 93-109.

[4] H. Tabatabai, Centrifuge modeling of underground structures subjected to blast loading, PhD Thesis, Department of Civil Engineering, University of Florida, 1987.

[5] A. De, T.F. Zimmie, T. Abdoun, and A. Tessari, Physical modeling of explosive effects on tunnels, Fourth International Symposium on Tunnel Safety and Security, Frankfart am Main, Germany, March 2010, pp 159-167.

[6] H-S. Shim, Response of piles in saturated soil under blast loading, Doctoral thesis, University of Colorado, Boulder, US, 1996.

[7] N.M. Nagy, E.A. Eltehawy, H.M. Elhanafy, and A. Eldesouky, Numerical modeling of geometrical analysis for underground structures, 13th international conference on aerospace science and aviation technology, Cairo, Egypt, 2009.

[8] M. Kumar, V.A. Matsagar, and K.S. Rao, Blast loading on semi buried structures with soil-structure interaction, proceeding of IMPLAST conference, Rhode Island, USA, 2010.

[9] Anirban De, Numerical simulation of surface explosions over dry, cohesionless soil, Computers and Geotechnics, 43, 2012, pp 72-79.

[10] M.D. Bolton, A.M. Britto, and T.P. White, Finite element analysis of a centrifuge model retaining wall embedded in overconsolidated clay. Computers and Geotechnics, 7 (4) (1989), pp 289-318.

[11] H. G. B. Allersma, R.B.J. Brinkgreve, and T. Simon, Centrifuge and numerical modeling of horizontally loaded suction piles, International Journal of Offshore and Polar Engineering, Volume 10 (3), 2000.

[12] Y. Kohgo, A. Takahashi, and T. Suzuki, FEM consolidation analysis of centrifuge test for rockfill dam during first reservoir filling, ASCE, Unsaturated soils, 2006, pp 2312-2323.

[13] E.A. Ellis, and S.M. Springman, Modeling of soil-structure interaction for a piled bridge abutment in plane strain FEM analyses, Computers and Geotechnics, 28 (2) (2001), pp 79-98.

[14] J. Chen, and S. Yu, Centrifugal and numerical modeling of a reinforced lime-stabilized soil embankment on soft clay with wick drains, Int. J. Geomech., 11(3) (2011), pp 167–173.

[15] S.P.G. Madabhushi, and S.K. Haigh, Finite element analysis of pile foundations subjected to pull-out, http://www2.eng.cam.ac.uk/~skh20/Udine.pdf

[16] LS-DYNA, Livermore software technology cooperation, LS-DYNA user's manual, version 971, 2007.

[17] J. Granier, C. Gaudin, S.M. Springman, P.J. Culligan, D. Goodings, B. Kutter, R. Phillips, M.F. Randolph, and L. Thorel, Catalogue of scaling laws and similitude questions in centrifuge modeling, International Journal of Physical Modelling in Geotechnics, 7 (3) (2007), pp 1-24.

[18] B.L. Kutter, and R.G. James, Dynamic centrifuge model tests on clay embankments, Geotechnique, 39 (1) (1989), pp 91-106.

[19] D.A. Jones, and E.D. Northwest, Effect of case thickness on the performance of underwater mines, DSTO Aeronautical and Martine Research laboratory, Melbourne, 1995.

[20] W.Y. Lee, Numerical modeling of blast induced liquefaction, DAI, 67, no. 06B, 3305, 2006.

[21] B.A. Lewis, Manual for LS-DYNA soil material model 147, Federal Highway Administration, FHWA-HRT-04-095, McLean, VA, 2004.

[22] P. Sherker, Modeling the effects of detonations of high explosives to inform blast-resistant design, Master thesis, the University at Buffalo, State University of New York, 2010.

[23] E. Lee, M. Finer, and W. Collins, JWL equations of state coefficients for high explosives, Lawrence Livermore Laboratory, University of California, California, 1973.